Analyst

Cite this: *Analyst*, 2012, **137**, 4766

www.rsc.org/analyst

PAPER

Migration behaviour of discontinuous buffers in capillary electrophoresis during protein enrichment†

Ting Li, Christina J. Booker and Ken K.-C. Yeung*

Received 26th April 2012, Accepted 1st August 2012
DOI: 10.1039/c2an35548e

Capillary electrophoresis (CE) is not only an effective separation technique, but can also serve as a sample preparation tool for enrichment and purification at sub-microliter sample volumes. Our approach is based on the use of a discontinuous buffer system consisting of an acid and a base (acetate and ammonium). Proteins and/or peptides with isoelectric points between the pH values of these two buffers will become stacked at the neutralization reaction boundary (NRB). To understand the mechanism of the NRB formation and the electrophoretic migration of various ions during the enrichment, we performed experiments using myoglobin and mesityl oxide to reveal the ion migration patterns at the buffer junction, and utilized Simul 5 to computer simulate the process. The simulated results closely resembled the experimental data, and together, they effectively revealed the characteristics of the discontinuous buffers. Importantly, the discovery allowed the manipulation of NRB behaviours by controlling the discontinuous buffer composition. To illustrate this, the removal of urea as an unwanted background molecule from the enriched protein sample was achieved based on the acquired information.

1. Introduction

Protein expression in biological systems spans over a wide range in concentration.[1,2] Without PCR-like methods for protein amplification, the sensitivity of analytical instrumentation imposes a real limiting factor, and thus, enrichment of analytes prior to separation and detection becomes a critical step in the discovery of low abundance proteins. For separations taking place in capillary- or microchannel-formats, online enrichment techniques based on electrophoresis are available, and they are reviewed in ref. 3–6. In general, the enrichment mechanism is based on an abrupt reduction of analytes' electrophoretic mobilities as they migrate across a buffer zone boundary. Such stacking behaviour can be induced by a change in local electric field due to differences in ionic conductivity. Alternatively, a pH change in buffer zones can be used to alter the mobilities of ionizable analytes. This approach is particularly effective for proteins and peptides due to their amphiprotic nature.

Different versions of pH-mediated in-capillary enrichment have been developed. Isotachophoretic stacking was reported to allow the injection of large volume protein samples prior to CZE.[7–9] Since the ionization of proteins is highly pH-dependent, buffered leading and terminating electrolytes (LE and TE) were necessary to control their electrophoretic mobility and ionic conductivity during ITP. In the cases where LE and TE of different pH values were used, a step-shaped pH gradient resulted at the ITP steady state, with the pH steps corresponding to the resolved protein zones.[10]

Alternatively to ITP, Britz-McKibbin and colleagues developed an enrichment technique based on a dynamic pH junction, which was created by injecting a sample plug prepared in a pH either higher or lower than the background electrolyte. The term *dynamic* referred to the short-lived nature of the pH-junction, which quickly dissipated after stacking to facilitate the separation of enriched analytes. Applications of this technique included small ionizable analytes,[11–14] peptides[15,16] and proteins.[17] In a similar approach to the dynamic pH junction, Cao and co-workers reported the use of a moving neutralization reaction boundary (NRB) for the enrichment of zwitterionic analytes.[18] The operating principle is analogous to the dynamic pH junction technique, where the sample is prepared in a pH different from the running buffer, and the analytes become stacked prior to dissipation of the pH junction and subsequent CZE separation. However, the reports by Cao *et al.* also focused on the theoretical development to understand the stacking mechanisms.[19–21] According to them, the velocity and direction of the NRB movement are determined by the relative flux of H^+ to that of OH^- at the NRB, which in turn depends on parameters including the ion mobility, ion concentration and local electric field.

Our group also reported in-capillary pH-mediated enrichment of proteins. A discontinuous buffer system, consisting of a pH 4.75 acetate buffer at the anode and a pH 9.25 ammonium buffer at the cathode, was employed to generate the required NRB for

Department of Chemistry and Department of Biochemistry, The University of Western Ontario, London, Ontario, Canada. E-mail: kyeung@uwo.ca; Tel: +1 (519) 661 2111

† Electronic supplementary information (ESI) available. See DOI: 10.1039/c2an35548e

stacking. This setup allowed the creation of a sharp, step-shaped pH junction, which was confirmed experimentally using UV-absorbing pH indicators.[22] The pH junction was shown to selectively enrich proteins and peptides with isoelectric points between the boundary pH values of the discontinuous buffers, using model proteins, myoglobin (pI 7.2), amyloglucosidase (pI 3.6) and cytochrome *c* (pI 10.6),[23] and peptides from the tryptic digestion of myoglobin.[24] Importantly, further to enrichment, the pH junction also served as a means of protein immobilization and facilitated in-capillary modifications of the enriched proteins, including proteolysis,[25] and purification to remove unwanted background ionic salts and buffer ions.[26,27]

To study the migration of ions in our discontinuous buffers during enrichment, we have relied on the direct approach of monitoring the movements of UV-absorbing ions with the online CE detector. This included measuring the electroosmotic flow (EOF) with mesityl oxide, displaying the pH profile with pH indicators,[22,23] and monitoring the migration of UV-absorbing molecules such as proteins or background salts and buffering ions to be removed.[26,27] However, the migration of the discontinuous buffer ions themselves (acetate and ammonium), being weakly or non-UV absorbing, could not be monitored in this way. A conductivity detector coupled to a CE instrument would be useful to monitor these optically inactive ions,[28,29] but unfortunately was not available to us.

An indirect approach to investigate ion migration behaviours in CE is computer modelling based on the theories describing electrophoretic processes. Computer simulation programs are available, have been used in many CE applications, and have recently been reviewed by Thormann *et al.*[30,31] Examples of recent dynamic simulation models are GENTRANS,[32–34] Simul 5,[35,36] and SPRESSO.[37,38] These computer models are based on partial differential equations in time and space (often in 1-D) that encompass electromigration including analyte charge and mobility, diffusion, and bulk flow to track the movement of each species in solution. These equations also incorporate the principles of electroneutrality, conservation of mass and charge, and dissociation–association equilibria of weak electrolytes and ampholytes. Both GENTRANS and Simul 5 have been applied to model systems consisting of pH junctions. However, GENTRANS is only available in the laboratories of the program developers at the Universities of Bern and Tasmania.[31,32] Simul 5, on the other hand, is free software offered by Professor Bohuslav Gaš for public online download. The first application of Simul 5 on the pH junction technique investigated the focusing mechanism of weakly acidic analytes at a dynamic pH boundary.[13] Simulations were used to optimize the enrichment with sample pH and injection length, and to examine the enrichment, separation, and identification of metabolites using a combination of dynamic pH-junction and transient cationic isotachophoresis (tCITP).[39] Ševčík and co-workers have also employed Simul 5 to explain the mechanism of stacking of weakly acidic analytes at a neutralization reaction boundary.[40]

Our group also previously reported the application of Simul 5 to model our discontinuous buffer system. In particular, it was applied to stimulate the migration behaviour of TRIS and phosphate during their removal, and to reveal the effect of phosphate on the migration of acetate and ammonium ions.[26] Also noteworthy was the observation of a slow moving NRB from the simulated results, as described by Cao *et al.*[20] However, this observation was not validated experimentally. In this manuscript, a systematic investigation on the migration behaviour of the buffering ions and protein analyte ions is presented with experimental data and corresponding simulations with Simul 5. Specifically, the effects of pH and concentration of the discontinuous buffers on the stability and movement of the NRB, and in turn the enrichment of proteins, are investigated. Understanding the ion migration around the pH junction allows us to assess the benefits and limitations of our pH junction technique, and is essential in developing future applications of in-capillary protein modifications.

2. Materials and methods

2.1 Apparatus

An Agilent 3D Capillary Electrophoresis (Palo Alto, CA, USA) instrument with a direct UV-visible absorbance detector was used for all CE experiments. Data were collected by the Agilent ^{3D}CE ChemStation software. Fused silica capillaries of 50 μm i.d. and 364 μm o.d. were purchased from Polymicro Technologies (Phoenix, AZ, USA). The capillaries were cut to a total length of 48.5 cm, with a length-to-detector of 40.0 cm and they were thermostatted to 25 °C during experiments.

A Bruker Reflex IV MALDI time-of-flight mass spectrometer (Billerica, MA, USA) equipped with a 337 nm nitrogen laser was used for mass spectral analyses.

2.2 Reagents

Deionized water (18.2 MΩ cm) from a Millipore water purification system (Bedford, MA, USA) was used to prepare all solutions. A 0.1 mM 1,2-dilauroyl-*sn-glycero*-3-phosphocholine (DLPC; Avanti Polar Lipids, Alabaster, AL, USA) solution was prepared in 20 mM tris(hydroxymethyl)aminomethane (TRIS; Aldrich, St. Louis, MO, USA) and 20 mM calcium chloride (Caledon Laboratories, Georgetown, ON, Canada), and the pH of this solution was adjusted to pH 7.2 by hydrochloric acid (EM Science, Gibbstown, NJ, USA). Mesityl oxide (MO; Aldrich) was used as a neutral marker to mark the original buffer junction. Acetic acid and ammonium hydroxide (EM Science, Gibbstown, NJ, USA) were used to make the buffer solutions. Myoglobin from horse heart (Sigma, St. Louis, MO, USA) was used as received. Urea (Sigma or EM Science) was used as received, and was added directly to the protein sample solutions.

α-Cyano-4-hydroxy-cinnamic acid (CHCA; Sigma) was purified in ethanol (Fisher Scientific, Nepean, ON, Canada) according to the recrystallization procedure provided by Sigma/Aldrich. HPLC grade acetone (Fisher) and HPLC grade methanol (Caledon) were used in preparing the CHCA matrix.

2.3 Protein enrichment and urea removal

New capillaries were washed by flushing (1 bar) with 0.1 M NaOH for 10 minutes, followed by water for 10 minutes. To minimize protein adsorption, a semi-permanent coating of DLPC was used to modify the capillary inner wall by flushing

(1 bar) with DLPC solution for 20 minutes. In between runs, the capillary coating was regenerated by flushing (1 bar) with DLPC solution for 10 minutes. The capillary was flushed (1 bar) with water for 5 minutes prior to storage. The DLPC coating was also reported to suppress the electroosmotic mobility to roughly 10^{-5} cm^2 V^{-1} s^{-1}, with the actual values determined by pH and composition of the background electrolyte.[41]

Our discontinuous buffers consisted of two buffers, an acidic buffer (acetate) and a basic buffer (ammonium). The acetate buffer was prepared using various concentrations of acetic acid (10 mM to 50 mM), with the pH adjusted (between 4.25 and 5.25) by adding an appropriate amount of ammonium hydroxide. Likewise, the ammonium hydroxide at various concentrations (10 mM to 50 mM) was adjusted to different pH values (from 8.75 to 10.25) with acetic acid to form the ammonium buffer. Myoglobin, at a concentration of 10 ng μL^{-1}, was prepared in the ammonium buffer. Unless otherwise stated, the enrichment was conducted as previously reported;[23] that is, the capillary was first filled with the myoglobin sample in ammonium buffer (1 bar). Then a constant voltage (30 kV) was applied with the acetate buffer placed at the inlet (anode) and the ammonium buffer placed at the outlet (cathode). For the urea removal experiment, 10 ng μL^{-1} myoglobin was prepared in ammonium buffer containing 1 M urea. All the CE results presented have been verified by triplicate experiments.

2.4 Simul 5

Simul 5 obtained online (web.natur.cuni.cz/~gas/) was used in all computer simulation experiments. Our discontinuous buffers system was input into Simul 5 as an isotachophoretic system, with a leading electrolyte (the basic buffer) and a terminating electrolyte (the acidic buffer). The acidic buffer of the discontinuous buffers was input as the anolyte, referred to as the TE, while the alkaline buffer was input as the catholyte or LE. Simul 5 uses different coloured traces to distinguish between the ammonium ions in the TE and that in the LE, likewise for acetate in the TE and acetate in the LE. For simplicity, the TE–LE traces of each of these ions were combined in the figures presented herein. Myoglobin was input into Simul 5 by tabulating the number and pK_a values of the acidic and basic amino acid residues in its sequence: 3.5 (*C*-terminal), 3.9 (aspartic acid), 4.1 (glutamic acid), 6.0 (histidine), 8.0 (*N*-terminal), 10.5 (tyrosine and lysine) and 12.5 (arginine). When the overall charge of the protein was positive, the experimentally determined mobility of myoglobin in the acidic buffer was used (1.9×10^{-4} cm^2 V^{-1} s^{-1}), and when the overall charge was negative, the mobility of myoglobin determined in the basic buffer (1.5×10^{-4} cm^2 V^{-1} s^{-1}) was entered.

To speed up the simulation, the capillary length was shortened by 10 times, from 48.5 cm to 48.5 mm. However, the electric field was maintained as constant; *i.e.*, the voltage was changed from 30 kV in 48.5 cm to 300 V in 48.5 mm. In Simul 5, the EOF is handled as a separate, user-defined entry, which does not directly affect the simulation besides moving the entire capillary content forward. Since the EOF was variable in this case due to the different buffer pH values, a zero EOF was used in all experiments for simplicity.

2.5 MALDI mass spectrometry

To facilitate MALDI MS analysis, a pressure of 50 mbar was applied to push the capillary content onto a MALDI mass spectrometry target plate, as previously described.[42] A 20 second deposition period was used to yield a spot volume of approximately 40 nL, and up to 10 sample spots were collected per CE experiment.

Layers of the CHCA matrix were pre-deposited on the target plate, prior to sample deposition from the capillary. The first CHCA layer was 0.350 μL of 5 mg mL^{-1} CHCA in acetone and methanol (4 : 1 by vol), followed by the three layers of 0.200 μL of saturated CHCA solution in water–methanol (3 : 2 by vol) and 0.1% TFA. The multiple layers of CHCA and TFA were required to acidify the sample which can contain basic buffers. All mass spectra of myoglobin were acquired in the positive ion, linear mode. Voltage settings were left at the preset instrument default settings by Bruker. Each mass spectrum was a sum of 20 spectra from individual laser shots. Igor Pro 6.2 (WaveMetrics, Lake Oswego, OR, USA) was used to process the data for presentation.

3. Results and discussion

3.1 Validation of simulation on the NRB

Even though Simul 5 was previously applied to model our discontinuous buffers,[26] the focus was on the removal of unwanted background ions, TRIS and phosphate. In this work, our interest is on the discontinuous buffer ions, ammonium and acetate, in particular how they play a role in the migration of the NRB and in turn the enriched myoglobin. Thus, the task of utmost importance is to validate the simulation on the NRB with experimental data.

Simul 5 simulation was performed on a discontinuous buffer system with [H^+] in the acid matching the [OH^-] in the base, namely 20 mM pH 4.25 acetate and 20 mM pH 9.75 ammonium, according to the conditions shown in Fig. 1A. Specifically, 20 mM acetic acid with 4.73 mM ammonium hydroxide was input as the anolyte, whereas 20 mM ammonium hydroxide with 4.73 mM acetic acid was entered as the catholyte. These concentrations resulted in the pH step-junction of pH 4.25 and 9.75 shown in the initial simulation setup ($t = 0$, green trace in Fig. 1B). A noteworthy observation is the nearly identical initial ionic conductivity between the two sides of the pH junction (black trace in Fig. 1B). To minimize the simulation time, a small plug, instead of a capillary full, of myoglobin was chosen as the sample zone (pink trace in Fig. 1B).

The predicted concentration profiles of various ions after 1000 s of voltage application are shown in Fig. 1C. Importantly, it predicted the continued presence of a sharp pH junction and the accumulation of myoglobin as a narrow band which coincided with this pH junction. The conductivity trace was no longer constant across the pH junction. A small drop was located on the anodic side next to the pH junction, which appeared to reflect the decrease in the acetate concentration. Finally, a shift in the pH junction position indicated a cathodic NRB movement.

To validate the simulation results, an enrichment experiment was performed with the same discontinuous buffer composition. In contrast to the starting conditions used in Simul 5, the entire

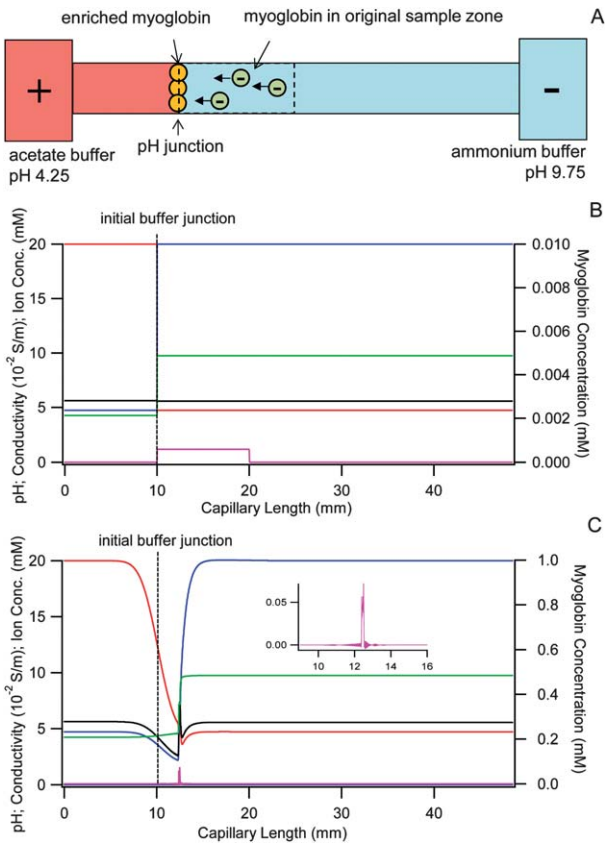

Fig. 1 (A) A schematic illustrating the capillary content at the starting condition for computer simulation. Yellow circles represent the analyte, myoglobin. Simulated conductivity, pH and ion concentration profiles at: (B) time = 0 s and (C) time = 1000 s. Acetate ion conc. (—), conductivity (—), ammonium ion conc. (—), pH (—), and myoglobin conc. (—). The inset displays a magnified view of the myoglobin peak.

capillary was initially filled with myoglobin prepared in the ammonium buffer. Hence, the pH junction was initiated between the alkaline buffer inside the capillary tip and the surrounding acidic buffer in the anodic reservoir. Another condition that was different between the simulation and experiment was the EOF. In Simul 5, the EOF was treated as zero, and thus the pH junction movement was solely a result of the moving NRB between the two buffers. In the actual experiment, a suppressed EOF existed in the DLPC-coated capillaries. Hence, the pH junction was also mobilized by the EOF, and therefore the apparent migration of the NRB/pH junction was a sum of the intrinsic NRB mobility and the EOF. To determine this EOF a plug of MO was injected at the anodic end of the capillary to mark the location of the initial acetate–ammonium buffer boundary (Fig. 2A).

Fig. 2B displays the absorbance signals recorded at 200 and 254 nm as the enriched myoglobin and MO passed the detection point. The inset of the figure is an enlarged view of the myoglobin signal showing the peak shape. In this particular trial, the myoglobin peak preceded the MO peak by approximately 2 minutes. However, the migration times of these peaks were found to vary between runs. The mean and standard deviation based on 20 replicates were 21.7 and 4.8 min for myoglobin, and 22.6 and 4.8 min for MO. The equal intensity in standard deviations

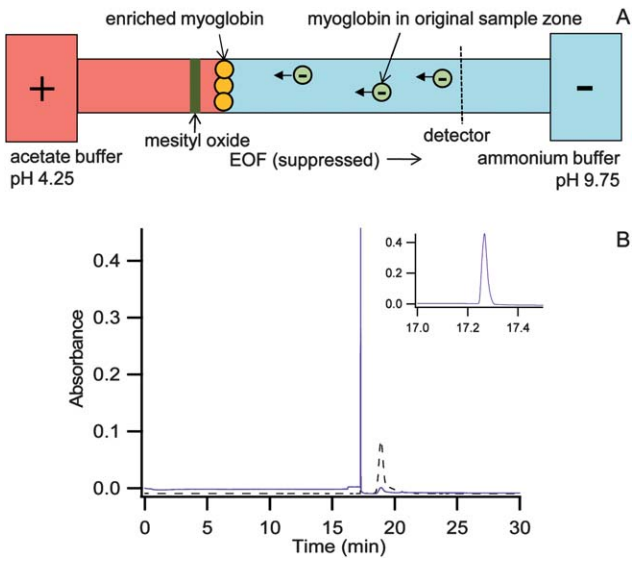

Fig. 2 (A) A schematic depicting a cathodic NRB during myoglobin enrichment. (B) UV absorbance signals recorded at 200 (—) and 254 nm (---) to reveal the presence of myoglobin and MO, respectively, during enrichment with discontinuous buffers of pH 4.25 and 9.75. The inset displays a magnified view of the myoglobin peak.

suggested that the variability of the migration times was caused predominantly by the EOF.

Presumably one would determine the electroosmotic mobility next based on the migration time of the MO. However, this was not feasible in this case due to the EOF dependency on pH. The EOF in a DLPC-modified capillary was previously determined to vary by pH, *i.e.*, 1×10^{-4} cm^2 V^{-1} s^{-1} in pH 9.75 ammonium buffer and 1×10^{-5} cm^2 V^{-1} s^{-1} in pH 4.25 acetate buffer.[27] In other words, a faster EOF occurred at the beginning of the run when the capillary was mostly filled with the pH 9.75 buffer. As the run proceeded, the EOF carried the pH 4.25 buffer into the capillary, and gradually slowed itself. Hence, such varying electroomostic mobility could not be calculated solely from the observed migration time of MO; and as a result, the exact NRB mobility could not be determined simply by subtraction. Instead, the difference in migration times ($t_{MO} - t_{myo}$) was determined for each of the 20 trials. An average of 0.9 min was obtained, with a standard deviation of 1.0 min. Such results at least allowed us to conclude a cathodic, near-zero, NRB movement, which in turn validated the simulated small cathodic NRB movement observed in Fig. 1C.

3.2 Discontinuous buffer pH

Our research on this discontinuous buffer system was initially conducted with pH 4.75 acetate and pH 9.25 ammonium buffers,[23] and more recently with pH 4.25 acetate and pH 9.75 ammonium buffers.[24,25,27] The pH values of these buffers were selected to generate equal concentrations of [H$^+$] and [OH$^-$], and thus, a near-zero NRB movement was expected. Additional buffers examined previously included phosphate, TRIS, formate and citrate. Successful myoglobin enrichment was only observed for two additional buffer pairs, pH 3.75 formate with pH 9.25 ammonium, and pH 4.75 acetate with pH 8.0 TRIS.[22] However, the NRB movements in these buffers were not determined at that time.

In this section, a systematic study on the effect of buffer pH on the NRB movement is presented. Simul 5 data are compared with experimental results obtained from discontinuous buffers of various pH combinations. In all simulations, the concentrations of the two buffers were kept at 20 mM, and the experimental conditions were set as those in Fig. 2A, with the only variable being the pH of the two buffers. Table 1 lists the pH combinations used for our simulations and experiments. The pH values were chosen to provide a wide range of $[H^+]/[OH^-]$ ratios, and thus large differences in the relative ion flux between H^+ and OH^-, in order to induce significantly different NRB movements. In all the simulation results obtained, pH step-junction profiles similar to that in Fig. 1C were observed. To illustrate the differences in NRB velocities, the positions of pH traces at $t = 1000$ s were superimposed in Fig. 3A, with the initial position ($t = 0$) marked by a dashed line. The pH traces on the right side of the dashed line indicate forward cathodic NRB movements, whereas pH traces on the left side indicate reverse anodic NRB movements.

To obtain the corresponding experimental data, myoglobin enrichment was conducted with the same list of discontinuous buffers in Table 1. In each case, a myoglobin peak and a MO peak were observed. As discussed, the NRB velocity and the varying electroosmotic mobility together determined the migration time of the myoglobin peak. To focus on changes in the NRB velocity, the myoglobin signals were shifted in time, in the *x*-axis direction, to align the MO peaks to 0 min (Fig. 3B). As a result, myoglobin peaks observed before the MO peaks indicate cathodic NRB movements, while myoglobin peaks detected after MO indicate anodic NRB movements.

The most important observation from comparing the simulated and experimental results was the identical order, from most anodic to most cathodic NRB movements. This again confirmed that Simul 5 was an excellent tool in predicting the ion migration behaviours during protein enrichment with our discontinuous buffers. Generally, the NRB moved in the cathodic direction when $[H^+]/[OH^-]$ was greater than 1, and moved in the anodic direction when $[H^+]/[OH^-]$ was less than 1. Larger NRB movements were observed when the difference between $[H^+]$ and $[OH^-]$ was greater. The only exception was the pH 4.25/10.25 buffer pair, where the NRB velocity was faster than predicted according to the order in $[H^+]/[OH^-]$ ratio. Likewise, for the buffer pair of pH 4.25/9.75, where $[H^+]$ was equal to $[OH^-]$, a small cathodic NRB displacement was predicted and observed. Under these two observations where pH alone could not explain the behaviours, one could attribute the results to the other two parameters that determine H^+ and OH^- flux, namely the mobility and local ionic conductivity. For instance, the mobility of the H^+ ($350\ m^2\ V^{-1}\ s^{-1}$) is higher than that of OH^- ($198\ m^2\ V^{-1}\ s^{-1}$).[43] The conductivity, according to Fig. 1C, was lower on the anodic side of the NRB than that on the cathodic side. These factors likely also contributed to the observed NRB movements.

Table 1 $[H^+]/[OH^-]$ ratios of various discontinuous buffer combinations

Acetate pH	Ammonium pH	$[H^+]$	$[OH^-]$	$[H^+]/[OH^-]$
4.25	8.75	5.6×10^{-5}	5.6×10^{-6}	10
4.25	9.25	5.6×10^{-5}	1.8×10^{-5}	3.1
4.25	9.75	5.6×10^{-5}	5.6×10^{-5}	1
4.25	10.25	5.6×10^{-5}	1.8×10^{-4}	0.31
4.75	9.75	1.8×10^{-5}	5.6×10^{-5}	0.31
5.25	9.75	5.6×10^{-6}	5.6×10^{-5}	0.1
5.25	10.25	5.6×10^{-6}	1.8×10^{-4}	0.031

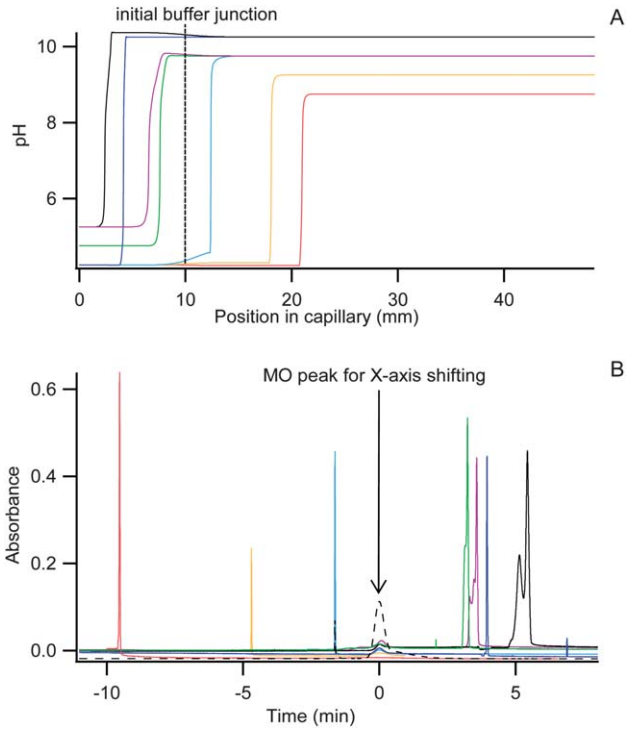

Fig. 3 (A) Simulated locations of pH junctions at 1000 s with discontinuous buffers of various pH combinations. (B) Experimental results of the enriched myoglobin peaks obtained with discontinuous buffers of various pH combinations. The traces were aligned to position the MO peaks at 0 min. The pH values of acetate/ammonium buffer were: 5.25/10.25 (—), 4.25/10.25 (—), 5.25/9.75 (—), 4.75/9.75 (—), 4.25/9.75 (—), 4.25/9.25 (—), 4.25/8.75 (—), and MO (---).

Another noteworthy observation in Fig. 3B was the different peak shapes of the enriched myoglobin. Sharp, single peaks resulted for four discontinuous buffer combinations, and broad split peaks were observed for three buffer pairs, namely pH 4.75/9.75, 5.25/9.75, and 5.25/10.25. Importantly, Simul 5 also predicted more gradual pH transitions, at the basic side of the junction, for these three buffer pairs (Fig. 3A). Furthermore, the broadening of the pH junction coincided with a large drop in conductivity in all three cases (ESI, Fig. S1†). Hence, we speculated that the proteins were stacked first by the conductivity rise as they approached the junction from the basic buffer, and subsequently focused a second time when they reached the centre of the pH junction, resulting in the observed peak splitting. This phenomenon illustrated the importance of background buffer ions and the effects they can have on the pH junction formation. Additional investigation into the role of the discontinuous buffer ions continues in the next section.

3.3 Discontinuous buffer concentration

Previous enrichment experiments in our laboratory with discontinuous buffers were typically performed at equal

concentrations of acetate and ammonium, 10 or 20 mM. In this section, the formation of a pH junction and the movement of a NRB were examined with pH 4.25 acetate and pH 9.75 ammonium, under various concentrations of acetate/ammonium, 10/10, 10/50, 50/10, and 50/50 mM. Simul 5 simulations were conducted with these four buffer pairs. Fig. 4A shows the pH junction locations and profiles after 1000 s of voltage application. It predicted significant cathodic NRB movements at buffer concentrations (acetate/ammonium) of 10/10 and 10/50 mM, and near-zero NRB movements at 50/10 and 50/50 mM.

Next, myoglobin enrichment experiments were performed using the same four buffer pairs. An injection of a MO plug was used again to mark the initial position of the acetate/ammonium interface for EOF determination. Triplicate experiments were conducted. In each case, a myoglobin peak and a MO peak were obtained (data not shown). As in Section 3.1, significant run-to-run variability in migration times due to EOF fluctuation was observed here. To best illustrate the differences in NRB movements obtained from the four buffer pairs, while accounting for run-to-run variability, the migration time differences between MO and myoglobin ($t_{MO} - t_{myo}$) from triplicates are shown in Fig. 4B. Positive values of $t_{MO} - t_{myo}$ indicate cathodic NRB movements, while negative values refer to NRB movements in the anodic direction. Taking run-to-run variation into account, the experimental data generally supported the Simul 5 results, that is, Simul 5 correctly predicted similarly significant cathodic NRB movements with buffer concentrations of 10/10 and 10/50 mM, and relatively slower NRB movements with the concentrations of 50/10 and 50/50 mM. While the direction of NRB movement at 50/50 mM was opposite to the simulated direction, such a NRB could be regarded as near-zero where the direction became less significant.

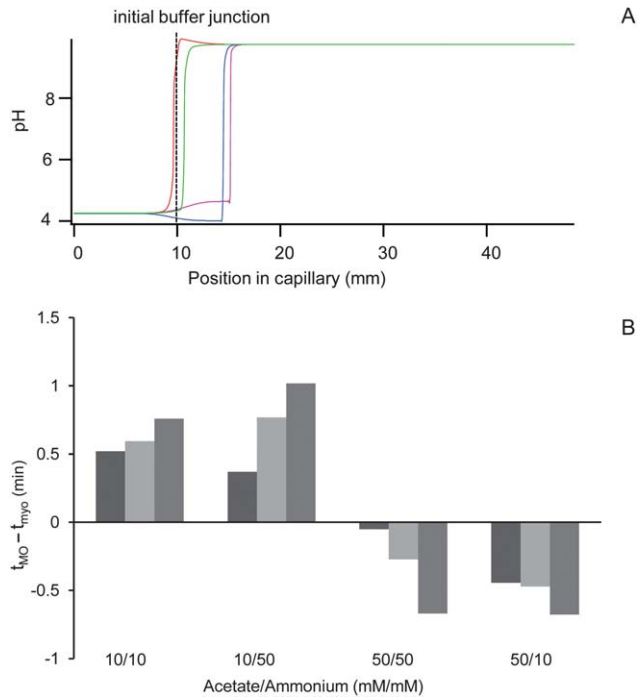

Fig. 4 (A) Simulated locations of pH junctions at 1000 seconds with discontinuous buffers of various concentrations (acetate/ammonium, mM/mM): 10/10 (—), 10/50 (—), 50/50 (—), and 50/10 (—). (B) The migration time differences between MO (t_{MO}) and myoglobin (t_{myo}) from triplicates (each bar represents one experiment) obtained at various discontinuous buffer concentrations.

Interestingly, based on the four buffer concentrations studied, it appeared that the NRB movement was mainly determined by the concentration of the acetate buffer, and less affected by the concentration of the ammonium buffer. After reviewing the full Simul 5 data, the conductivity profile near the pH junction appeared to explain the NRB movements observed (ESI, Fig. S2†). In the buffer pairs of 10/10 and 10/50 mM, the conductivity on the anodic (acid) side of the pH junction was lower, and thus promoted higher H^+ flux and cathodic NRB movements. In the 50/50 mM buffers, the conductivity profile was symmetrical across the pH junction, and a negligible NRB movement was obtained. Finally, for the 50/10 mM buffer pair, a higher conductivity was obtained on the anodic side, which resulted in an anodic, albeit very small, NRB movement.

Finally, by comparing the changes in NRB movements influenced by the buffer pH (Fig. 3) and those induced by buffer concentrations (Fig. 4), one can generalize that the buffer pH is a more effective parameter in manipulating and controlling the NRB compared to the buffer concentration.

3.4 Protein enrichment and purification from urea

The above experimental and simulated results provide the information for one to understand and control the NRB movement in discontinuous buffers of acetate and ammonium. In this section, we will illustrate how a fast moving NRB can actively mobilize the enriched proteins away from the original sample zone, which can be beneficial for purifying samples containing unwanted background molecules that bear a neutral net charge. For illustration, urea will be used as a model neutral background molecule. It is a common protein denaturant that unfolds proteins by disrupting the non-covalent interactions,[44,45] and can be used to elute affinity-captured proteins.[46] However, the presence of urea can suppress the mass spectral signals of proteins, likely due to a decrease of evaporation efficiency.[47]

Solid phase capture of proteins and peptides is the most common approach of urea removal.[48–50] Herein, a non-sorptive-based, sub-microliter volume purification is proposed by performing protein enrichment with discontinuous buffers that generate a moving NRB. Such NRB movement is expected to carry the enriched protein molecules far away from the unwanted neutral background present in the initial sample zone.

The sample consisted of 10 ng μL^{-1} myoglobin and 1 M urea, prepared in the ammonium buffer. It was injected to fill the capillary at the beginning of the run, to provide an injection volume of *ca.* 1 μL (Fig. 5A). In this setup, an anodic NRB movement was required to move the enriched myoglobin away from the sample zone. Based on the results in Fig. 3, the largest anodic NRB movement was recorded with acetate buffer at pH 5.25 and ammonium buffer at pH 10.25, and thus they were selected for this experiment (concentration at 20 mM). Fig. 5B displays the UV absorption signal recorded during the enrichment and purification. Urea, at high concentration, absorbs significantly at 200 nm, and was detected as a long rectangular plug between 0 and 13 min as the capillary content was mobilized

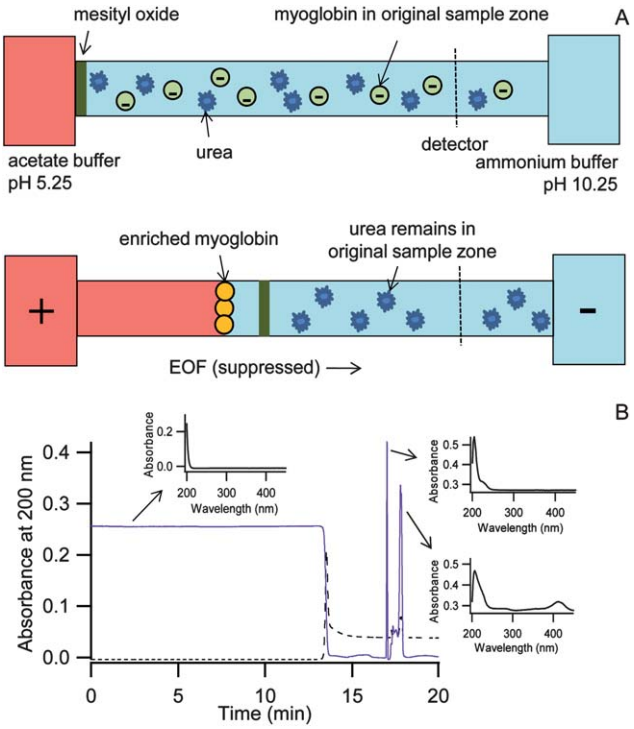

Fig. 5 (A) Schematics illustrating the experimental setup and proposed ion migration behaviours during myoglobin enrichment and simultaneous urea removal. (B) UV absorbance signals at 200 (—) and 254 nm (---) during the experiment. Insets display the UV absorption spectra of the indicated regions.

by the residual EOF. Subsequently, two peaks were recorded, at approximately 17 and 18 min. To help determine their identity, UV absorption spectra were collected and are shown as insets in Fig. 5B. The characteristic heme absorption at 408 nm indicated the second peak at 18 min for myoglobin. Hence, a 5 min separation between the myoglobin peak and the urea zone resulted, which was estimated to be roughly 250 nL in volume. This large separation was highly advantageous later when performing fraction collection for offline MALDI MS analysis.

To determine the origin of the second peak at 17 min blank experiments were conducted without the presence of myoglobin, using four different lots of urea, BCBD7141V, 057K01321, 109K00821 (Sigma) and 41058130 (EM Science). Similar peaks as the one at 17 min in Fig. 5B were observed in three cases, with varying peak heights and widths. This indicated that the signal likely originated from impurities or degradation products in the reagents.

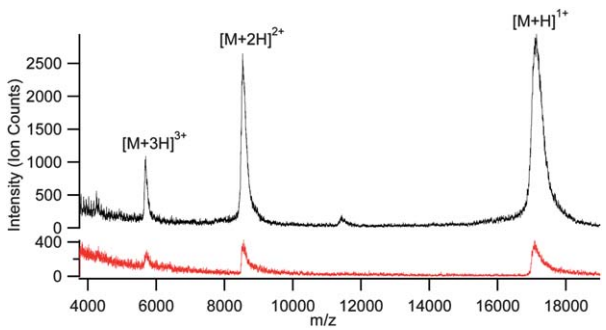

Fig. 6 MALDI mass spectra of myoglobin: from an untreated 100 ng μL^{-1} sample in 1 M urea (—) and from a 10 ng μL^{-1} sample in 1 M urea after enrichment and urea removal (—).

To illustrate the benefit of our protein enrichment and purification technique, offline MALDI MS analysis was conducted. Following protein enrichment, one end of the capillary was repositioned to outside of the CE instrument. Pressure was applied to push the capillary content out of the capillary as fractions of *ca.* 40 nL droplets. These droplets were spotted onto the MALDI MS target pre-deposited with CHCA. The mass spectrum obtained from the fraction that contained most of the myoglobin is shown as the black trace in Fig. 6. For comparison, an untreated sample consisting of 100 ng μL^{-1} myoglobin and 1 M urea was spotted from a capillary in the same way for MS analysis (shown as the red trace in Fig. 6). Despite the higher concentration, the untreated sample resulted in lower MS signal intensities. This illustrated that the enrichment and purification of myoglobin was successful by our technique. It also facilitated the subsequent offline MALDI MS analysis, and substantial improvement in the quality of the mass spectrum was evident.

4. Conclusion

CE, with the use of suitable discontinuous buffers, can serve as an effective tool for sample preparation for proteins in small sample volumes. A selection of discontinuous buffers, and their pH conditions, had previously been studied and demonstrated to work effectively. However, a systematic study to look at the effect of buffer composition on the migration of ions within the discontinuous buffers has not been reported. In this paper, the use of Simul 5 together with experimental validation for such an investigation was reported. The results concluded that the pH junction formed from discontinuous buffers in CE behaves as a NRB, with its mobility mostly determined by the pH of the buffers, and to a lesser extent, by the buffer concentrations. Simul 5 correctly predicted the direction and velocity of the NRB, and therefore is invaluable in understanding the migration of various ions in the discontinuous buffers. These findings allowed us to effectively manipulate the behaviour and properties of the NRB, and in turn facilitated the simultaneous myoglobin enrichment and the removal of urea in the sample background. An enhancement in MS signals was illustrated by an offline MALDI mass spectral analysis.

Acknowledgements

The Natural Sciences and Engineering Research Council of Canada (NSERC) and the University of Western Ontario financially supported this work. The Canada Foundation for Innovation and the Ontario Innovation Trust funded the Bruker Reflex IV mass spectrometer. The Agilent capillary electrophoresis instrument was funded by the Academic Development Fund Program of Western.

References

1 N. L. Anderson and N. G. Anderson, *Mol. Cell. Proteomics*, 2002, **1**, 845–867.
2 G. L. Corthals, V. C. Wasinger, D. F. Hochstrasser and J. C. Sanchez, *Electrophoresis*, 2000, **21**, 1104–1115.

3 M. C. Breadmore, M. Dawod and J. P. Quirino, *Electrophoresis*, 2011, **32**, 127–148.
4 L. A. Kartsova and E. A. Bessonova, *J. Anal. Chem.*, 2009, **64**, 326–337.
5 Z. Malá, A. Šlampová, P. Gebauer and P. Boček, *Electrophoresis*, 2009, **30**, 215–229.
6 C. A. Nesbitt, H. X. Zhang and K. K. C. Yeung, *Anal. Chim. Acta*, 2008, **627**, 3–24.
7 F. Foret, E. Szoko and B. L. Karger, *J. Chromatogr., A*, 1992, **608**, 3–12.
8 F. Foret, E. Szoko and B. L. Karger, *Electrophoresis*, 1993, **14**, 417–428.
9 T. J. Thompson, F. Foret, P. Vouros and B. L. Karger, *Anal. Chem.*, 1993, **65**, 900–906.
10 R. A. Mosher, P. Gebauer, J. Caslavska and W. Thormann, *Anal. Chem.*, 1992, **64**, 2991–2997.
11 P. Britz-McKibbin, G. M. Bebault and D. D. Y. Chen, *Anal. Chem.*, 2000, **72**, 1729–1735.
12 P. Britz-McKibbin and D. D. Y. Chen, *Anal. Chem.*, 2000, **72**, 1242–1252.
13 J. B. Kim, P. Britz-McKibbin, T. Hirokawa and S. Terabe, *Anal. Chem.*, 2003, **75**, 3986–3993.
14 A. S. Ptolemy and P. Britz-McKibbin, *Analyst*, 2008, **133**, 1643–1648.
15 M. R. N. Monton, K. I. M. Nakanishi, J.-B. Kim and S. Terabe, *J. Chromatogr., A*, 2005, **1079**, 266–273.
16 K. Imami, M. R. N. Monton, Y. Ishihama and S. Terabe, *J. Chromatogr., A*, 2007, **1148**, 250–255.
17 E. A. Bessonova, L. A. Kartsova and A. U. Shmukov, *J. Chromatogr., A*, 2007, **1150**, 332–338.
18 C.-X. Cao, Y.-Z. He, M. Li, Y.-T. Qian, M.-F. Gao, L.-H. Ge, S.-L. Zhou, L. Yang and Q.-S. Qu, *Anal. Chem.*, 2002, **74**, 4167–4174.
19 C. Cao, W. Zhang, L. Fan, J. Shao and S. Li, *Talanta*, 2011, **84**, 651–658.
20 C. X. Cao, L. Y. Fan and W. Zhang, *Analyst*, 2008, **133**, 1139–1157.
21 W. Zhu, W. Zhang, L.-Y. Fan, J. Shao, S. Li, J.-L. Chen and C.-X. Cao, *Talanta*, 2009, **78**, 1194–1200.
22 K. Jurcic, C. A. Nesbitt and K. K. C. Yeung, *J. Chromatogr., A*, 2006, **1134**, 317–325.
23 C. A. Nesbitt, J. T. M. Lo and K. K. C. Yeung, *J. Chromatogr., A*, 2005, **1073**, 175–180.
24 C. A. Nesbitt, K. Jurcic and K. K. C. Yeung, *Electrophoresis*, 2008, **29**, 466–474.
25 C. A. Nesbitt and K. K. C. Yeung, *Analyst*, 2009, **134**, 65–71.
26 C. J. Booker, S. Sun, S. Woolsey, J. S. Mejia and K. K. C. Yeung, *J. Chromatogr., A*, 2011, **1218**, 5705–5711.
27 C. J. Booker and K. K. C. Yeung, *Anal. Chem.*, 2008, **80**, 8598–8604.
28 R. M. Guijt, C. J. Evenhuis, M. Macka and P. R. Haddad, *Electrophoresis*, 2004, **25**, 4032–4057.
29 P. Kubáň and P. C. Hauser, *Electrophoresis*, 2009, **30**, 176–188.
30 W. Thormann, M. C. Breadmore, J. Caslavska and R. A. Mosher, *Electrophoresis*, 2010, **31**, 726–754.
31 W. Thormann, J. Caslavska, M. C. Breadmore and R. A. Mosher, *Electrophoresis*, 2009, **30**, S16–S26.
32 M. C. Breadmore, R. A. Mosher and W. Thormann, *Anal. Chem.*, 2006, **78**, 538–546.
33 Q. L. Mao, J. Pawliszyn and W. Thormann, *Anal. Chem.*, 2000, **72**, 5493–5502.
34 W. Thormann, C. X. Zhang, J. Caslavska, P. Gebauer and R. A. Mosher, *Anal. Chem.*, 1998, **70**, 549–562.
35 B. Gaš, M. Jaroš, V. Hruška, I. Zuskova and M. Stedry, *LC GC Eur.*, 2005, **18**, 282–289.
36 V. Hruška, M. Jaroš and B. Gaš, *Electrophoresis*, 2006, **27**, 984–991.
37 Y. Chou and R. J. Yang, *J. Chromatogr., A*, 2010, **1217**, 394–404.
38 M. Bercovici, S. K. Lele and J. G. Santiago, *J. Chromatogr., A*, 2009, **1216**, 1008–1018.
39 R. Lee, A. S. Ptolemy, L. Niewczas and P. Britz-McKibbin, *Anal. Chem.*, 2007, **79**, 403–415.
40 K. Vitkova, J. Petr, V. Maier, J. Znaleziona and J. Ševčík, *Electrophoresis*, 2010, **31**, 2771–2777.
41 J. M. Cunliffe, N. E. Baryla and C. A. Lucy, *Anal. Chem.*, 2002, **74**, 776–783.
42 K. Jurcic and K. K. Yeung, *Electrophoresis*, 2009, **30**, 1817–1827.
43 P. Vanýsek, in *CRC Handbook of Chemistry and Physics*, ed. W. H. Haynes, CRC Press Online, 92nd edn, 2011–2012.
44 W. Kauzmann, *Adv. Protein Chem.*, 1959, **14**, 1–63.
45 C. N. Pace, *Methods Enzymol.*, 1986, **131**, 266–280.
46 D. A. Kaiser, P. J. Goldschmidtclermont, B. A. Levine and T. D. Pollard, *Cell Motil. Cytoskeleton*, 1989, **14**, 251–262.
47 J. P. Antignac, K. de Wasch, F. Monteau, H. De Brabander, F. Andre and B. Le Bizec, *Anal. Chim. Acta*, 2005, **529**, 129–136.
48 Y. S. Huh, K. Yang, Y. K. Hong, Y. S. Jun, W. H. Hong and D. H. Kim, *Process Biochem.*, 2007, **42**, 649–654.
49 P. R. Sudhir, H. F. Wu and Z. C. Zhou, *Anal. Chem.*, 2005, **77**, 7380–7385.
50 Y. Xu, M. L. Bruening and J. T. Watson, *Mass Spectrom. Rev.*, 2003, **22**, 429–440.